Published in final edited form as:
J Neurosurg. 2003 September ; 99(2 0): 206–213.

Tethering of the spinal cord in mouse fetuses and neonates with spina bifida

Dorothea Stiefel, MD[1,2], **Takashi Shibata, MD**[1,3,4], **Martin Meuli, MD**[2], **Patrick G. Duffy, MD**[3], and **Andrew J. Copp, MD PhD**[1]

[1]Neural Development Unit, Institute of Child Health, University College London, UK [2]Department of Pediatric Surgery, University Children's Hospital Zurich, Switzerland [3]Department of Paediatric Urology, Great Ormond Street Hospital for Children NHS Trust, London, UK [4]Department of Urology, Hokkaido University, Sapporo, Japan

Abstract

Object—Tethering of the spinal cord is a well known complication in humans with *spina bifida* (SB) *aperta* or *occulta*. Its pathogenesis consists of a pathological fixation of the spinal cord resulting in traction on the neural tissue which, in turn, leads to ischemia and progressive neurological deterioration. Although well established in humans, the phenomenon of cord tethering has not been described in animal models of SB.

Methods—A fetal mouse model with naturally occurring, genetically determined SB was produced by generating double mutants between the *curly tail* (*ct*) and *loop-tail* (*Lp*) mutant strains. Microdissection, labelling with DiI, immunohistochemistry for neurofilaments, hematoxylin and eosin staining of histological sections and whole mount skeletal preparations were used in the comparison of mutant and normal fetuses.

Conclusions—Normal fetuses exhibit the onset of progressive physiological ascent of the spinal cord from embryonic day (E) 15.5. Spinal cord ascent results, by E18.5, in spinal nerve roots that pass *caudo*-laterally from the spinal cord towards the periphery. In contrast, fetuses with SB exhibit spinal cord tethering that results, at E18.5, in nerve roots that run in a *cranio*-lateral direction from the spinal cord. The region of closed spinal cord immediately cranial to the SB lesion exhibits marked narrowing, late in gestation, suggesting that a potentially damaging stretch force is applied to the spinal cord by the tethered SB lesion. This mouse model provides an opportunity to study the onset and early sequelae of spinal cord tethering in SB.

Keywords

Neural tube; myelomeningocele; embryo; mutant; kyphosis; scoliosis

Corresponding author: Andrew Copp, Neural Development Unit, Institute of Child Health, University College London, 30 Guilford Street, London WC1N 1EH, UK Tel. +44 20 7829 8893; Fax: +44 20 7831 4366; a.copp@ich.ucl.ac.uk.

INTRODUCTION

Physiological ascent of the spinal cord begins after gestational day 54 in the human embryo, with the conus medullaris reaching the level of L1-3 by three months postpartum [9;13]. Following this stage, the finding of a conus below L3 is suggestive of low fixation of the spinal cord, which may be symptomatic in the so-called "tethered cord syndrome" [9;20;26].

Spinal cord tethering is characterised by symptoms with progressive intensity such as backpain due to scoliosis, incontinence resulting from a neurogenic bladder, and numbness, weakness or pain of the lower extremity and foot deformity as a result of progressive sensory and motor deficit [3;6;14-16;22-25;29;34]. Spinal cord tethering has been described mostly in children and adolescents [4;6;14;15;19;22-24;32-34], particularly in patients with spinal dysraphism (*spina bifida aperta* or *occulta*). Cutaneous stigmata, such as dimples, hairy patches, abnormal pigmentation and lipomas, are often found at the site of the spinal abnormality [15-17;24;29;30;32]. However, cord tethering may also occur in patients without cutaneous signs, thus presenting a truly occult spinal dysraphism [20;29].

The various conditions leading to tethering of the spinal cord include a thickened or tight filum terminale, abnormalities of the conus medullaris such as syringomyelia, diplomyelia, diastematomyelia, dermoids or intradural cysts [5;14;15;24;29;30;33] and the various forms of SB *aperta* or *occulta*. Even though the etiology of spinal cord tethering can be variable, its pathogenesis appears more uniform, involving pathological fixation of the spinal cord in an abnormal (usually caudal) position [3;24;26;29;30;33]. This elicits traction with daily body movements, leading to repeated extension and distortion of the spinal cord and, finally, to ischemia, progressive neurological deterioration and even skeletal deformity [24].

The aim of our study was to investigate the fetal ascent of the spinal cord in the mouse as, to our knowledge, neither fetal ascent nor tethering of the spinal cord have been documented in a suitable animal model. We chose a mouse model with naturally occurring SB, enabling a comparison between fetuses and neonates with and without SB. We determined the time of onset of the spinal cord ascent and documented findings of tethering and its early sequelae. In particular, we describe a compensational stretching mechanism of the closed part of the spinal cord in SB animals, as a consequence of the tethering of the open spinal lesion.

MATERIALS AND METHODS

Mouse strains

The *loop-tail (Lp)* mutation is an autosomal recessive cause of severe neural tube closure defects (craniorachischisis) with heterozygote effects including occasional SB and tail flexion defects [27]. The *curly tail (ct)* mutation is an autosomal recessive, partially penetrant cause of mouse SB [12]. Mice carrying both *loop-tail* and *curly tail* mutations (*Lp*/+, *ct/ct)* have severe SB in almost 100% of cases (Pavlovska and Copp, unpublished).

Collection of fetuses/newborns

Mice were maintained on a 12 h light, 12 h dark cycle (lights on from 07.00 to 19.00). Overnight matings between doubly heterozygous *loop-tail/curly tail* males (*Lp*/+, *ct*/+) and

homozygous *curly tail* females (+/+, *ct/ct*) were checked for vaginal plugs the following morning, the day of finding a copulation plug being designated embryonic day 0.5 (E0.5). Litters were collected at intervals between E11.5 and E18.5, as well as on postnatal day one (P1). Animals with SB were compared with their phenotypically normal littermates. Pregnant females were culled by cervical dislocation, and fetuses were dissected in Dulbecco's modified Eagle's medium (DMEM, Gibco, BRL, Life Technologies, Ltd., Paisley, U.K.) containing 10% fetal calf serum. The extra-embryonic membranes were removed, the fetuses were rinsed in phosphate buffered saline (PBS) and then culled on a frozen metal plate before fixation. Newborn pups were culled by an overdose (10 ml/kg body weight) of Midazolam (Hypnovel®, Roche Products Ltd, Hertfordshire, U.K.), mixed 1:1 with Fentanyl (Hypnorm®, Janssen Pharmaceutica, Beerse, Belgium) and diluted to 50% in distilled water. All experiments with mice were performed with appropriate licensing under the Animals (Scientific Procedures) Act, 1986 of the UK Government.

General morphology

E13.5 to E18.5 fetuses and postnatal day 1 pups (n = 35; 2-4 of each phenotype at each age) were fixed in Bouin's solution (Sigma) for 2-7 days, depending on age. After serial dehydration, they were embedded in paraffin wax and sectioned transversely at 8 μm thickness. Sections were dewaxed with Histo-Clear (National Diagnostics), serially rehydrated to distilled water, stained with Ehrlich's hematoxylin and eosin for 10 and 5 minutes respectively, dehydrated and mounted in DPX. Photographic documentation (for all specimens) was performed using colour reversal film on light microscopes (Zeiss, Stemi SV 11 and Axiophot).

Microdissection

After dorsal laminectomy, E18.5 fetuses (n = 2 with SB and 2 control) were placed in supine position, and the vertebral bodies were removed so that the spinal cord was completely freed from the vertebral column. This procedure enabled visualisation of the intact dorsal root ganglia and the spinal cord with its spinal nerve roots, especially the portion of the sensory roots connecting the dorsal root ganglia with the spinal cord.

DiI labelling

After laminectomy, the dorsal root ganglia and their respective spinal roots at L6 and S1 were identified in E18.5 fetuses (n = 3 with SB, 3 controls). To visualise the sensory nerve roots between the dorsal root ganglia and the dorsal sensory horn, crystals of DiI (1,1′-dioctadecyl-3,3,3′,3′-tetramethylindocarbocyanine perchlorate; Molecular Probes), a substance with an exclusively lipophilic character, were dissolved in dimethylformamide (2.5 mg/ml) prior to injection into the L6 and S1 dorsal root ganglia using a fine glass needle connected to an air pump. After injection, specimens were fixed at 4°C overnight in 4% paraformaldehyde in PBS (4% PFA), followed by incubation at 37°C for 2 to 3 weeks in order to allow the diffusion of DiI from the injection site along the axons.

Immunohistochemistry on sections

E12.5 to E18.5 fetuses and postnatal day 1 pups (n = 27; 1-3 of each phenotype at each age) were fixed in 4% PFA for 2-7 days, depending on age. They were dehydrated through an ethanol series and embedded in paraffin wax. Sections were cut at 8 μm thickness in a parasagittal plane, dewaxed, rehydrated and unmasked with Declere (Cell Marque) in a microwave oven. Endogenous peroxidase was quenched by incubation in 0.6% H_2O_2/Tris buffered saline (TBS; 0.05 M Tris, 0.15 M NaCl, pH 7.6) for 7.5 minutes and non-specific epitopes were blocked by exposure to 10% fetal calf serum (FCS) in 0.5% Triton X-100 in TBS. Monoclonal anti-neurofilament 68 antibody (Sigma N5139, mouse IgG_1) was applied overnight at 4°C, diluted 1:400 in TBS containing 1% FCS and 0.5% Triton X-100. The following day the sections were washed in TBS/1% FCS/0.5% Triton X-100 and then exposed for 1 hour to secondary biotinylated rabbit anti-mouse IgG antibody (DAKO), diluted 1:500 in the same solution. Several washes in TBS were followed by reaction with streptavidin-biotinylated horseradish peroxidase (DAKO) for 30 minutes at room temperature. Coloration of the neurofilaments was obtained by 3,3′-diaminobenzidine (DAB, Sigma). Control sections, in which the primary antibody was substituted by 1% FCS/TBS were negative in all cases.

Immunohistochemistry on whole mount preparations

E13.5 to E18.5 fetuses (n = 28; 1-3 of each phenotype at each age) were eviscerated and those older than E15.5 were also deskinned. After fixation in 4% PFA for at least 48 hours, fetuses were bleached in 6% H_2O_2 in PTX (PBS + 1% Triton X-100) for 30 minutes to 2 hours, depending on age. After several washes in PTX, fetuses were incubated for 3-5 hours in a blocking buffer solution (1 mg/ml bovine serum albumin, 5% heat inactivated sheep serum in PTX) to quench endogenous peroxidase and to block non-specific epitopes. Monoclonal anti-neurofilament 68 antibody was added to the solution, diluted 1:100, and incubation was continued for 7-10 days at 4°C on a rocking plate, followed by washes in PTX for 2 days. The secondary biotinylated rabbit anti-mouse IgG antibody was diluted 1:250 in blocking buffer solution and applied on a rocking plate for 5-7 days. Specimens were washed in PTX for 2 days, incubated in a solution containing streptavidin-biotinylated horseradish peroxidase for 2 days, washed again in PTX for 2 days and then rinsed several times in 0.1 M Tris-HCl (pH 7.4), followed by exposure to DAB and enhancement of staining with tap water. Fetuses were rinsed in dH_2O followed by 2 washes in PBS, serially dehydrated in methanols, then cleared and stored in methylsalicylate.

Whole body skeletal preparation

E14.5 to E18.5 fetuses and postnatal day 1 pups (n = 80; 3-10 of each phenotype at each age) were eviscerated and deskinned, then fixed in 4% PFA for several days. They were placed in Alcian Blue solution for 6 days at 4°C, rehydrated, transferred into Alizarin Red solution for 3 hours and then exposed to a series of glycerol-potassium-hydroxide solutions to clear the surrounding soft tissue before storage in 100% glycerol at room temperature.

RESULTS

Matings between doubly heterozygous (*Lp*/+, *ct*/+) males and homozygous *curly tail* (+/+, *ct/ct*) females generated litters containing fetuses with three different phenotypes: lumbosacral SB of varying size together with a curly tail (92/272 fetuses studied; 34.0%), curly tail alone (25.5%) and normal tail/spine (40.5%)(Fig. 1A-F).

Abnormal angulation of spinal nerve roots in fetuses with SB

Microdissection of the L6/S1 level in E18.5 normal fetuses showed spinal nerve roots running *caudo*-laterally from the spinal cord towards the periphery (Fig. 2A). Conversely in SB littermates the direction of the spinal nerve roots was *cranio*-lateral from the SB region of the spinal cord (Fig. 2B). To identify more clearly the microdissected dorsal root ganglia with their respective sensory nerve roots, dissolved DiI crystals were injected into L6/S1 dorsal root ganglia. After several weeks' incubation, normal E18.5 fetuses showed sensory nerve roots running *caudo*-laterally from the spinal cord at the level of the L2-3 intervertebral space to the dorsal root ganglia L6/S1 indicating a physiological ascent of the spinal cord of 3 to 4 vertebrae (Fig. 2C). In contrast, littermates with a large SB lesion showed L6/S1 nerve roots running *cranio*-laterally from the spinal cord. This effect was most pronounced at the cranial end of the SB lesion (Fig. 2D).

Changing angulation of spinal nerves with increasing gestation

In order to assess the time course of spinal cord ascent, fetuses were processed for neurofilament immunostaining. Sections from both normal and SB fetuses at E12.5 to E14.5 showed spinal nerve roots running perpendicularly from the spinal cord to the periphery, at all levels (Fig. 3A-F). After E14.5 the angle changed to an oblique direction, but the angle of the nerve roots was opposite in control and SB animals. Normal fetuses showed a *caudo*-lateral direction of nerve roots from the spinal cord ("pine tree-shaped" pattern, Fig. 3G), whereas SB fetuses exhibited a *cranio*-lateral direction of nerve roots from the spinal cord ("V-shaped" pattern), an effect that was most pronounced at the cranial end of the SB lesion (Fig. 3I). Whole mount neurofilament preparations confirmed that the conus medullaris and the filum terminale of normal fetuses are well distinguishable, reaching the vertebral level of S3/4 in normal fetuses by E18.5 (Fig. 3H). Whole mount neurofilament staining of E18.5 fetuses with SB did not yield clear results, owing to the degenerative changes underway in the SB lesion by this gestational stage (data not shown).

Progressive thinning of the closed spinal cord in SB animals with increasing gestation

In order to determine whether tethering of the SB also affects other parts of the spinal cord, fetuses were processed for histological analysis. At E13.5, sagittal sections of SB specimens showed an intact closed region of spinal cord, cranial to the SB lesion, which had the same diameter as in normal littermates (Fig. 4A,B). By E16.5, however, the distal end of the closed spinal cord in SB animals exhibited a slightly tapered appearance (data not shown) and, as gestation progressed, this tapering became increasingly marked so that, by E18.5, the spinal cord region cranial to the SB appeared markedly attenuated (Fig. 4D). At P1, however, this tapering was no longer visible, as the SB lesion had by then completely degenerated, releasing its tethering effect (Fig. 4F).

Skeletal lordosis and kyphosis at the site of the SB lesion before and after the onset of the spinal cord ascent

In humans, the presence of a tethered cord can be associated with exacerbation of scoliosis. Whole mount skeletal preparations at E14.5, a day before the onset of the spinal cord ascent, showed an even curvature of the spine in normal fetuses. In contrast, all SB littermates examined showed lordotic and kyphotic changes in the region of the lower back (site of the SB lesion) and the tail (data not shown). At all stages through P1 skeletal alterations were observed in the vertebral column in SB animals, usually presenting as a cranial lordosis followed by a distal kyphosis (Fig. 5B). Scoliotic changes did not occur. Normal fetuses maintained an even curvature of the spine throughout this period (Fig. 5A).

Post-natal consequences of SB in the mouse model

Although not the main focus of the study, it was noted that mice with SB invariably progressed to birth, but rarely survived beyond the neonatal period. Demise of neonates with SB resulted from hemorrhage at the lesion site, with consequent severe anemia and weakness which compromised the ability of the pups to compete with healthy littermates for maternal care and nutrition. Paralysis and loss of sensation in the lower extremities was documented in some pups with large SB lesions (D. Stiefel, in preparation). Hence, although mice with SB in this mouse model do not generally survive beyond the neonatal period, they do exhibit many of the features of human newborns with SB.

DISCUSSION

In human embryos, closure of the neural tube in the spinal region is completed around gestational day 30 [9]. At day 45 the spinal cord still shows the same length as its surrounding vertebral column, leading to a perpendicular course of the spinal nerve roots leaving the spinal cord. Thereafter, the very terminal end of the spinal cord undergoes morphogenetic changes, with formation of the fibrous filum terminale by about day 54 [9]. This process leads to an indirect ascent of the conus medullaris within the vertebral column to a level of S5 [13], but without changing the perpendicular angulation of the spinal nerve roots [9]. Beyond this time point, the ascent of the conus is attributed to true differences in growth rate between the spinal cord and the surrounding vertebrae, thus leading to an increasingly oblique (caudo-lateral) course of the nerve roots as they pass from the spinal cord to the intervertebral foramina [9]. Between weeks 12 and 24/25, the conus medullaris shows a significant variation of level between individuals [13] but, by 24 weeks of gestation, it usually lies at S1 [9] or above S1 [13]. At birth the conus has reached L2-3 [9], or L3 [13] and, by 1-3 months postpartum, the adult level of intervertebral space L1-2 [9] or L2-3 [13] is reached.

In contrast to the well documented physiological ascent of the spinal cord in human fetuses, the ascent of the spinal cord in individuals with myelomeningocele is poorly understood, having been described in relatively few studies. In a study of dysraphic fetuses, Barson showed that, beyond the gestational age of 9 weeks, spinal nerve roots within closed segments of the spinal cord become progressively angulated in a caudo-lateral direction whereas nerve roots immediately cranial to the myelocele pass in a cranio-lateral fashion to the intervertebral foramina [2]. Surprisingly, the same phenomenon was observed even in

cervical myelomeningocele where obliquely running nerves are unexpected, even in the case of the physiological ascent of the spinal cord. Fetuses in this study showed an additional Arnold Chiari type II malformation, which might have been the reason for traction of the spinal nerves, and thus for their changing angulation.

A tethered cord is a well known complication of human dysraphism. It may be caused by various conditions such as thickened filum terminale, lipoma, dermoid or myelo(meningo)cele [3;14;16;22;25;30]. The latter, following postnatal surgical closure, is by far the most frequent etiology [5;19], with tethering reportedly occurring in 100% [3;4], 95% [5] or 78% [33] of cases. Considering this high frequency, it is rather surprising that only a low incidence of symptomatic tethering has been reported. Selber [26]cited a 29% occurrence of tethered cord syndrome in adults, whereas in children symptomatic tethering was said to occur in 38% [5], more than 27% [18], 19% [3], 15% [30] and even 0% [4] of myelomeningocele cases.

The tethered cord, seen in individuals with myelomeningocele after postnatal closure, is usually a secondary effect of scar tissue formation at the site of the operation [1;3;14;21;30]. In contrast, cord tethering may be a primary finding in individuals with SB *occulta*, where the latter is often only diagnosed following the onset of symptoms of tethering [17;29]. There is only one report of spinal cord tethering occurring *prior* to postnatal myelomeningocele repair [33], similar to the findings in our mouse model. The lack of such reports might be attributed to the fact that the tethered cord is not a clinical feature commonly looked for in newborns with myelomeningocele, because its diagnosis does not change the therapeutic approach, nor the indication for surgery.

In the present study of a mouse model, we found that fetal ascent of the spinal cord begins at E15.5 in both normal and SB fetuses. Prior to E15.5, the nerve roots run perpendicularly to the spinal cord whereas later in gestation they run obliquely from the spinal cord (Fig. 6). Strikingly, however, normal fetuses exhibit nerve roots running *caudo*-laterally from the spinal cord, whereas fetuses with SB exhibit *cranio*-laterally running nerves. Thus, SB appears to prevent the physiological ascent of the spinal cord owing to pathological fixation of the primary malformed SB to the surrounding tissue, leading to the appearance of a tethered cord. Furthermore, we find that cord tethering affects the morphology of the portion of closed spinal cord immediately proximal to the SB lesion, which progressively elongates and tapers, apparently as a compensatory stretching mechanism. As a result of this localised cord elongation, nerve roots cranial to the lesion become gradually less obliquely angled (Fig. 6).

Over-extension of the spinal cord may cause axonal damage directly, and as an indirect effect of decreased oxygenation of the neural tissue, through ischemia and metabolic deficiency. Both effects could contribute to the atrophy and decrease in diameter observed in the distal part of the closed spinal cord in our study. A similar finding, of an atrophic spinal cord, was reported in 44% of humans with tethered cord syndrome [4]. A few studies have produced experimental spinal cord traction in order to simulate the tethered cord syndrome [8;10;11;31;34], and all conclude that traction of the spinal cord produces metabolic dysfunction and ischemia of the spinal cord.

If metabolic deficiency and ischemia are indeed elicited by a tethered, over-stretched spinal cord, progressive neuronal injury is likely [34] with progressive sensorimotor deficit, as often observed in humans with tethered cord [5;14;24;25;30;32]. The mouse model also shows a neurological deficit in late gestation, with the level of the deficit correlating closely with the size of the open SB (D. Stiefel, in preparation). However, the neurological deficit in the mice does not involve more proximally located spinal nerves, perhaps because tethering in the mouse is only of short duration (E15.5 to E18.5), in contrast to the long-term nature of tethered cord syndrome in humans, with its progressive development of sensorimotor deficit. Alternatively, the assessment techniques used to detect neurological deficit in mouse fetuses may be too insensitive to detect partial sensorimotor weakness or numbness, findings that are typical for progressive tethered cord syndrome.

Other mechanisms that may lead to over-stretched, tethered nerve roots could include abnormal curvature of the spine. Our animal model of SB shows various grades of kyphosis and lordosis throughout gestation, defects that originate as early as E13.5 or E14.5, *prior* to the onset of the spinal cord ascent. This would argue that the abnormal spinal curvature is unlikely to cause the progressive tethering but is more likely a result of progressive cord tethering, as often described in humans [5;18;21;23-26].

In conclusion, our finding of spinal cord tethering in an experimentally tractable mouse model of SB offers a route towards a more in-depth understanding of the clinically important phenomenon of spinal cord tethering and its early sequelae. Potential future studies with the model include determining the time course of neural degeneration in the exposed SB lesion, the contribution of tethering-induced stretch versus exposure to amniotic fluid in the pathogenesis of neural degeneration, and the relative onset of ischemia, metabolic dysfunction and axonal/neuronal injury in the tethered cord. The contribution of cord tethering to the pathogenesis of hindbrain herniation and hydrocephalus is also an area for future study. Preliminary results from fetal surgery for human SB demonstrate a lower incidence of hydrocephalus postnatally, suggesting that untethering of the SB lesion may contribute to minimisation of hindbrain herniation [7;28]. It will be instructive to determine the relationship between cord tethering and hindbrain herniation in the mouse SB model.

ACKNOWLEDGEMENTS

We thank Dr Saadi Ghatan for valuable comments on the manuscript. This work was supported by a research fellowship from the University of Zurich (D. Stiefel) and by the Wellcome Trust and the Medical Research Council, UK (A. Copp).

Grant support: University of Zurich, Switzerland, Research Fellowship (D. Stiefel); Wellcome Trust, UK, Programme Grant 051690 (A. Copp)

REFERENCES

1. Banta JV. The tethered cord in myelomeningocele: should it be untethered? Dev.Med Child Neurol. 1991; 33:173–176. [PubMed: 2015987]
2. Barson AJ. Spina bifida: the significance of the level and extent of the defect to the morphogenesis. Dev.Med.Child Neurol. 1970; 12:129–144. [PubMed: 4911460]
3. Begeer JH, Meihuizen de Regt MJ, HogenEsch I, et al. Progressive neurological deficit in children with spina bifida aperta. Z.Kinderchir. 1986; 41(Suppl 1):13–15. [PubMed: 3811614]

4. Bono R, Inverno M, Botteon G, et al. Clinical features and MR imaging in children with repaired myelomeningocele. Ital.J Neurol.Sci. 1993; 14:553–559. [PubMed: 8282527]
5. Brezner A, Kay B. Spinal cord ultrasonography in children with myelomeningocele. Dev.Med Child Neurol. 1999; 41:450–455. [PubMed: 10454228]
6. Bruce DA, Schut L. Spinal lipomas in infancy and childhood. Childs Brain. 1979; 5:192–203. [PubMed: 378579]
7. Bruner JP, Tulipan N, Paschall RL, et al. Fetal surgery for myelomeningocele and the incidence of shunt-dependent hydrocephalus. JAMA. 1999; 282:1819–1825. [PubMed: 10573272]
8. Cusick JF, Myklebust J, Zyvoloski M, et al. Effects of vertebral column distraction in the monkey. J Neurosurg. 1982; 57:651–659. [PubMed: 7131066]
9. Dias, MS. Myelomeningocele. In: Choux, M.; DR, C.; H, AD.; W, ML., editors. Pediatric Neurosurgery. Churchill Livingstone; 1999. p. 33-59.
10. Dolan EJ, Transfeldt EE, Tator CH, et al. The effect of spinal distraction on regional spinal cord blood flow in cats. J Neurosurg. 1980; 53:756–764. [PubMed: 7441335]
11. Fujita Y, Yamamoto H. An experimental study on spinal cord traction effect. Spine. 1989; 14:698–705. [PubMed: 2772718]
12. Gruneberg H. Genetical studies on the skeleton of the mouse. VIII. Curly tail. J.Genet. 1954; 52:52–67.
13. Hawass ND, el Badawi MG, Fatani JA, et al. Myelographic study of the spinal cord ascent during fetal development. AJNR Am J Neuroradiol. 1987; 8:691–695. [PubMed: 3113205]
14. Herman JM, McLone DG, Storrs BB, et al. Analysis of 153 patients with myelomeningocele or spinal lipoma reoperated upon for a tethered cord. Presentation, management and outcome. Pediatr.Neurosurg. 1993; 19:243–249. [PubMed: 8398848]
15. Hoffman HJ, Hendrick EB, Humphreys RP. The tethered spinal cord: its protean manifestations, diagnosis and surgical correction. Childs Brain. 1976; 2:145–155. [PubMed: 786565]
16. Hoffman HJ, Taecholarn C, Hendrick EB, et al. Management of lipomyelomeningoceles. Experience at the Hospital for Sick Children, Toronto. J Neurosurg. 1985; 62:1–8. [PubMed: 3964839]
17. Mapstone TB. Management of tethered spinal cord. Neurosurgery Quarterly. 1994; 4:82–91.
18. McLone DG. Continuing concepts in the management of spina bifida. Pediatr.Neurosurg. 1992; 18:254–256. [PubMed: 1476932]
19. McLone DG. The adult with a tethered cord. Clin.Neurosurg. 1996; 43:203–209. [PubMed: 9247804]
20. McLone, DG. Occult dysraphism and the tethered spinal cord. In: Choux, M.; DiRocco, C.; Hockley, AD., et al., editors. Pediatric Neurosurgery. Churchill Livingstone; 1999. p. 61-100.
21. McLone DG, Herman JM, Gabrieli AP, et al. Tethered cord as a cause of scoliosis in children with a myelomeningocele. Pediatr.Neurosurg. 1990; 16:8–13. [PubMed: 2133414]
22. McLone DG, Naidich TP. Laser resection of fifty spinal lipomas. Neurosurgery. 1986; 18:611–615. [PubMed: 3714009]
23. Pierz K, Banta J, Thomson J, et al. The effect of tethered cord release on scoliosis in myelomeningocele. J Pediatr.Orthop. 2000; 20:362–365. [PubMed: 10823605]
24. Reigel DH, Tchernoukha K, Bazmi B, et al. Change in spinal curvature following release of tethered spinal cord associated with spina bifida. Pediatr.Neurosurg. 1994; 20:30–42. [PubMed: 8142280]
25. Sarwark JF, Weber DT, Gabrieli AP, et al. Tethered cord syndrome in low motor level children with myelomeningocele. Pediatr.Neurosurg. 1996; 25:295–301. [PubMed: 9348149]
26. Selber P, Dias L. Sacral-level myelomeningocele: long-term outcome in adults. J Pediatr.Orthop. 1998; 18:423–427. [PubMed: 9661844]
27. Strong LC, Hollander WF. Hereditary loop-tail in the house mouse. J.Hered. 1949; 40:329–334.
28. Sutton LN, Adzick NS, Bilaniuk LT, et al. Improvement in hindbrain herniation demonstrated by serial fetal magnetic resonance imaging following fetal surgery for myelomeningocele. JAMA. 1999; 282:1826–1831. [PubMed: 10573273]

29. Tadmor R, Ravid M, Findler G, et al. Importance of early radiologic diagnosis of congenital anomalies of the spine. Surg.Neurol. 1985; 23:493–501. [PubMed: 3885450]
30. Tamaki N, Shirataki K, Kojima N, et al. Tethered cord syndrome of delayed onset following repair of myelomeningocele. J Neurosurg. 1988; 69:393–398. [PubMed: 3404237]
31. Tani S, Yamada S, Knighton RS. Extensibility of the lumbar and sacral cord. Pathophysiology of the tethered spinal cord in cats. J Neurosurg. 1987; 66:116–123. [PubMed: 3783242]
32. Vernet O, O'Gorman AM, Farmer JP, et al. Use of the prone position in the MRI evaluation of spinal cord retethering. Pediatr.Neurosurg. 1996; 25:286–294. [PubMed: 9348148]
33. Vogl D, Ring-Mrozik E, Baierl P, et al. Magnetic resonance imaging in children suffering from spina bifida. Z.Kinderchir. 1987; 42(Suppl 1):60–64. [PubMed: 3324544]
34. Yamada S, Zinke DE, Sanders D. Pathophysiology of "tethered cord syndrome". J Neurosurg. 1981; 54:494–503. [PubMed: 6259301]

Europe PMC Funders Author Manuscripts

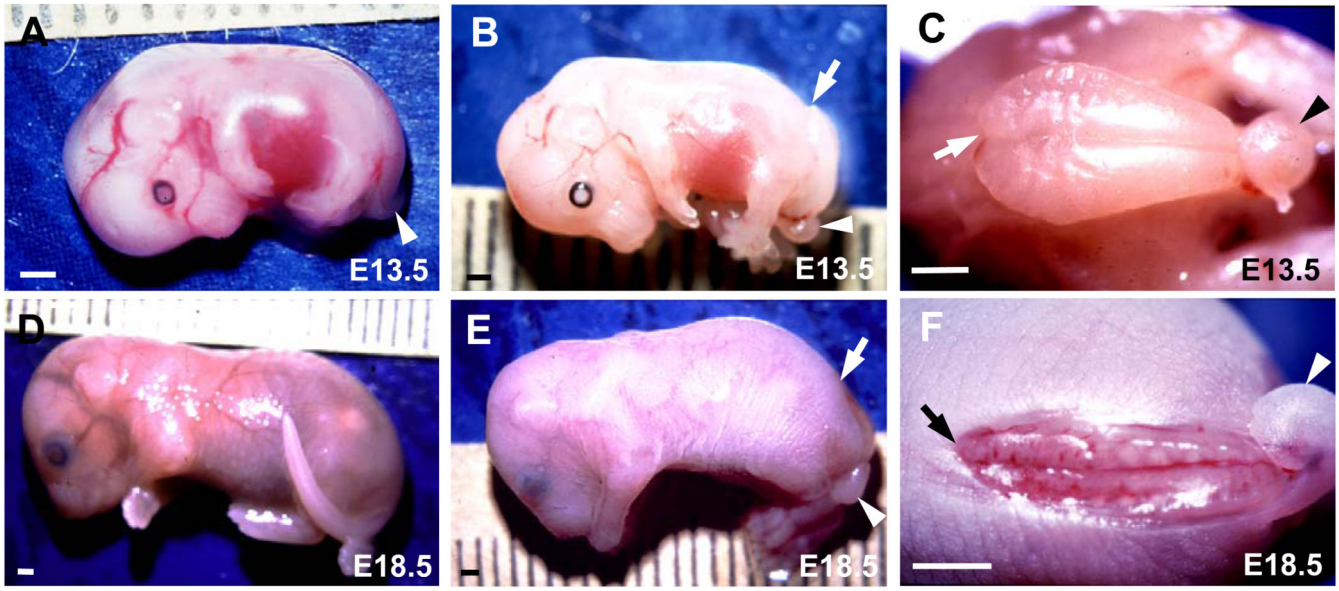

Figure 1. Appearance of spina bifida (SB) in mouse fetuses

Fetuses with curly tail only (A), SB plus curly tail (B,C,E,F) or normal tail/spine (D) at E13.5 (A-C) and E18.5 (D-F). Arrowheads indicate curled tails (A,B,C,E,F), while arrows point to the cranial end of the open SB lesion (B,C,E,F). (C) and (F) are magnified dorsal views of the fetuses in (B) and (E) respectively. Note the bulging SB lesion (B,C) at E13.5 compared with the flattened, degenerating lesion (E,F) at E18.5. Scale bars: 1 mm.

Europe PMC Funders Author Manuscripts

Europe PMC Funders Author Manuscripts

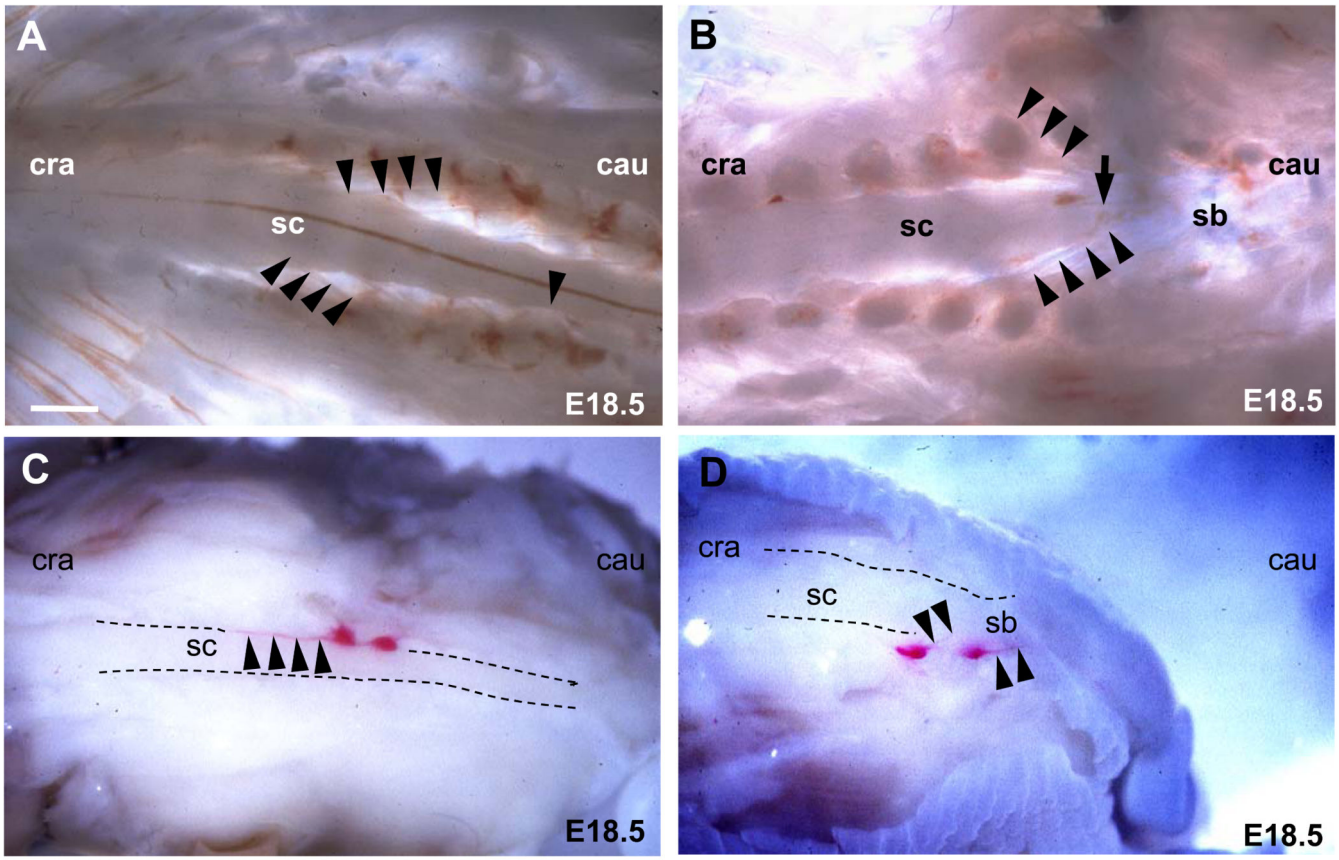

Figure 2. Abnormal angulation of spinal nerve roots in whole mount SB fetuses

(A,B) Dorsal view of microdissected E18.5 normal (A) and SB (B) fetuses. Cranial is to the left and caudal is to the right. The cranial end of the SB lesion (B) is marked with an arrow. Arrowheads trace the course of individual spinal nerve roots running from the spinal cord to the periphery. (C,D) DiI-labelled L6/S1 dorsal root ganglia (arrows) and their respective sensory nerve roots (arrowheads) in E18.5 fetuses. Dorsal view of right sided ganglia in a normal fetus (C) and dorsolateral view of left sided ganglia in a SB fetus (D). Abbreviations: cau, caudal; cra, cranial; sc, spinal cord; sb, spina bifida. Scale bars: 240 μm (A,B), 400 μm (C,D).

Europe PMC Funders Author Manuscripts

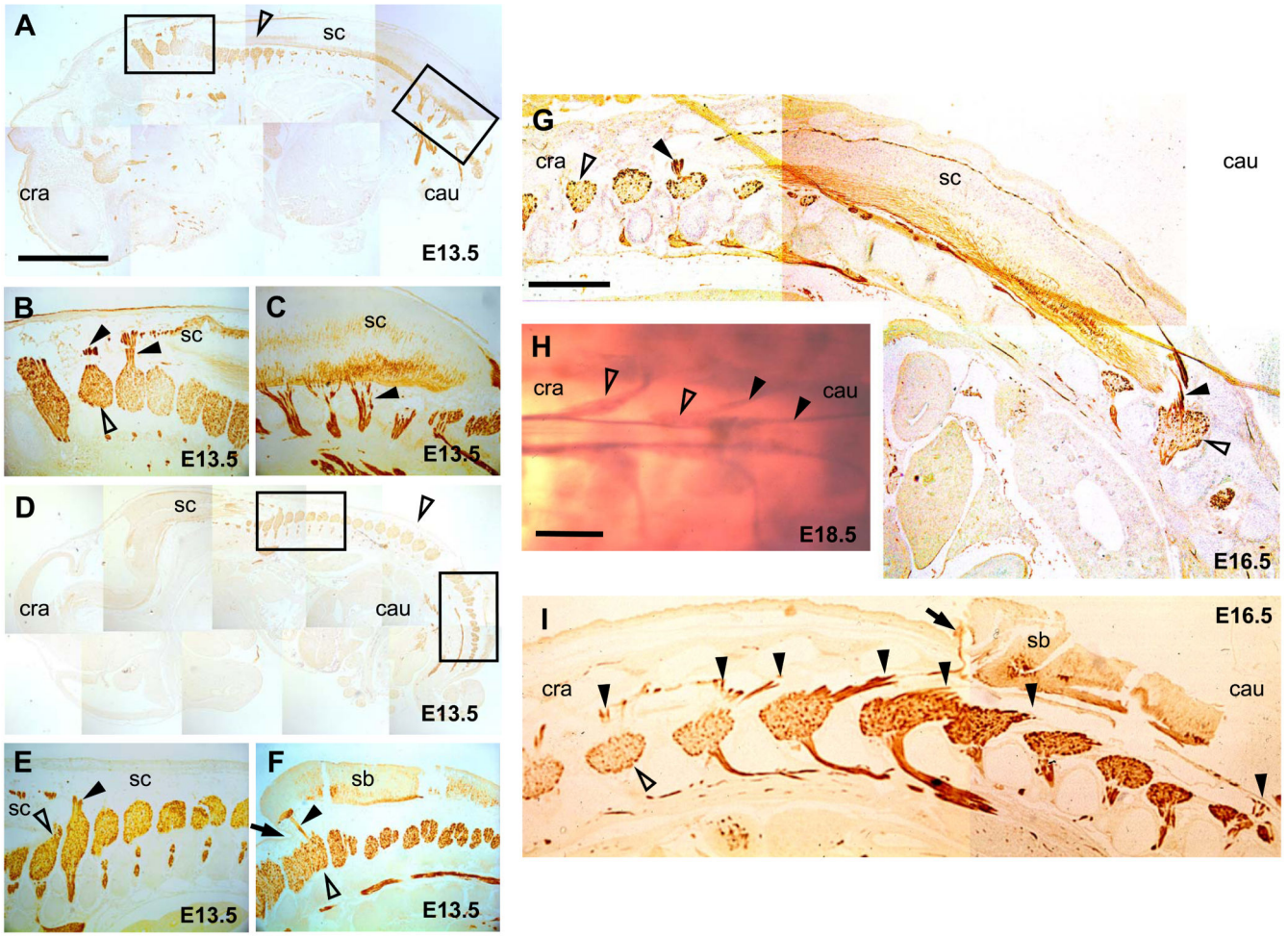

Figure 3. Abnormal angulation of spinal nerve roots in SB fetuses: neurofilament staining

Sagittal histological sections of normal (A-C,G) and SB (D-F,I) fetuses at E13.5 (A-F) and E16.5 (G,I) immunostained for neurofilaments. Cranial is to the left, caudal to the right. (B,C) and (E,F) are magnifications of boxed areas in (A) and (D), respectively. Open arrowheads mark dorsal root ganglia and closed arrowheads indicate spinal nerve roots. The arrows in (F) and (I) indicate the cranial end of the SB lesion. (H) Whole mount neurofilament immunostaining of a normal E18.5 fetus showing a dorsal view of the conus medullaris (arrow) with the filum terminale and the dorsal root ganglia (open arrowheads). Note the caudo-lateral direction of the nerve roots (closed arrowheads) leaving the spinal cord. Abbreviations: cau, caudal; cra, cranial; sc, spinal cord; sb, spina bifida. Scale bars: 200 μm (A,D), 500 μm (B,C,E,F), 475 μm (G,I), 455 μm (H).

Europe PMC Funders Author Manuscripts

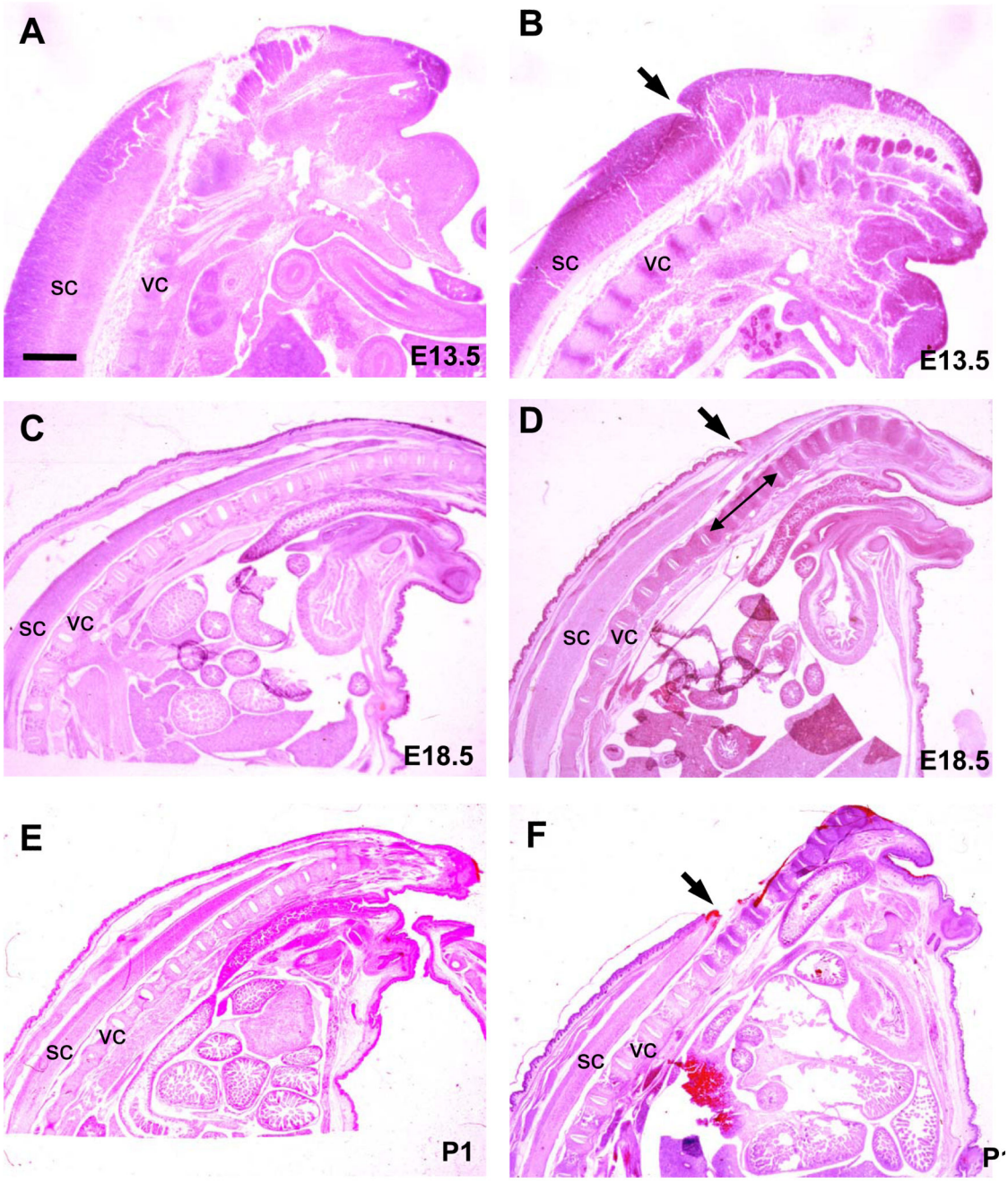

Figure 4. Stretching of the closed spinal cord immediately cranial to the SB lesion

Hematoxylin and eosin stained sagittal histological sections of normal (A,C,E) and SB (B,D,F) fetuses at E13.5 (A,B), E18.5 (C,D) and P1 (E,F). The end of the tail is to the right. Arrows indicate the cranial end of the SB lesion (B,D,F). Double headed arrow (in D) indicates region of spinal cord narrowing just cranial to SB lesion. Abbreviations: sc, spinal cord; vc, vertebral column. Scale bar: 4.2 mm (A,B), 1 mm (C-F).

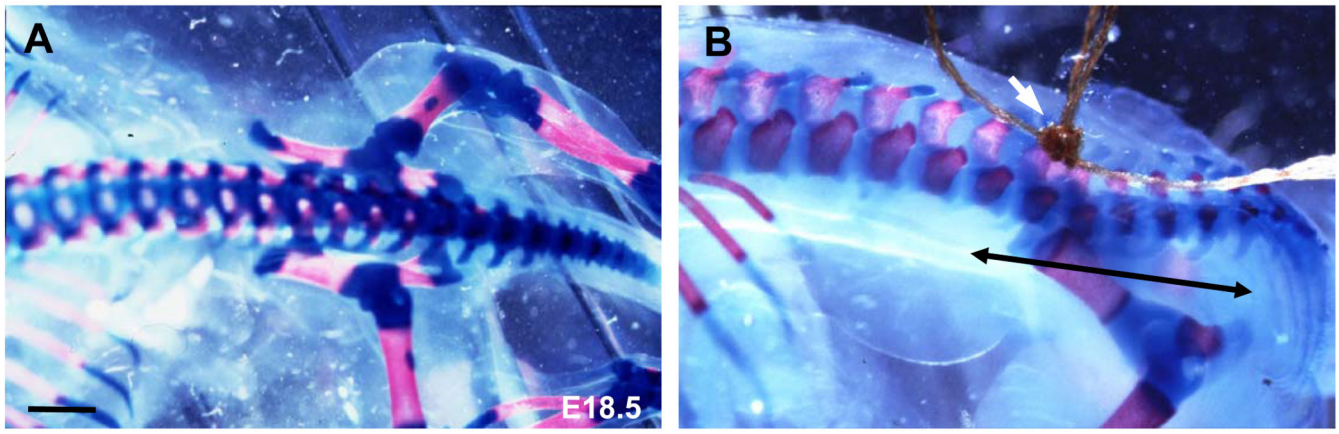

Figure 5. Kypho-lordotic deformity of the vertebral column in SB fetuses

Skeletal preparations of the lumbar spinal region in a dorsolateral view of E18.5 mouse fetuses. Cranial is to the left, caudal to the right. Bone is stained red and cartilage is blue. Note the even curvature of the spine in a normal fetus (A) as opposed to the kypho-lordotic spinal deformity in a SB fetus (B). Double headed arrow marks the region of the SB lesion, whose cranial end has been marked with a single suture (white arrow). Scale bar: 480 μm (A,B).

Europe PMC Funders Author Manuscripts

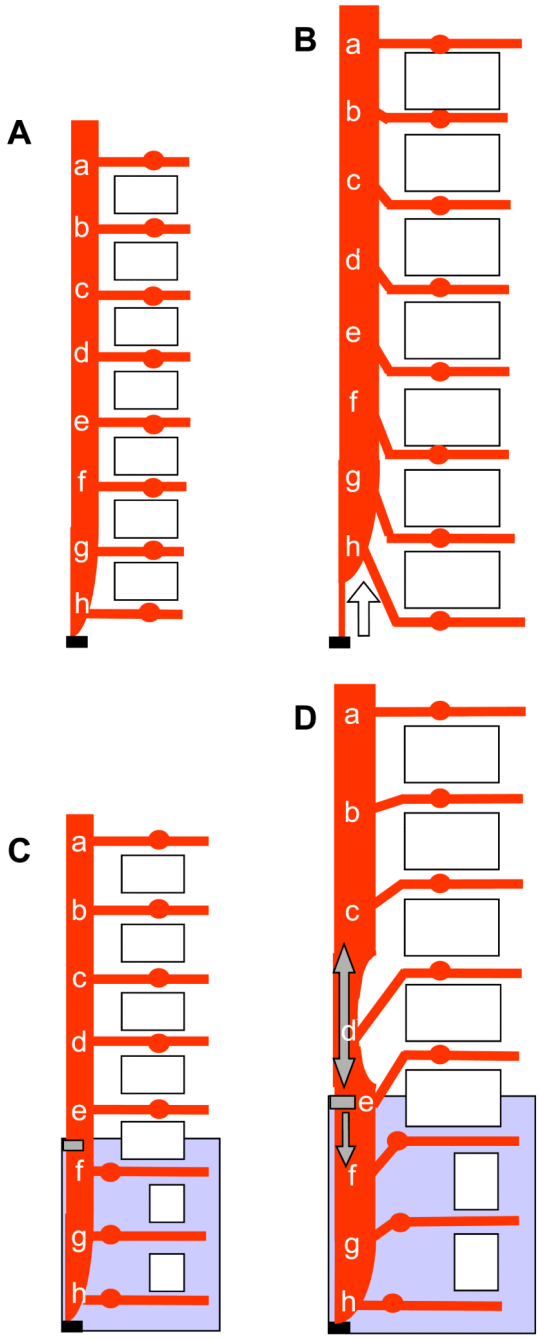

Figure 6. Summary of spinal cord ascent in normal (A,B) and SB (C,D) mouse fetuses with increasing gestation

The anatomy is depicted before (A,C) and after (B,D) the onset of spinal cord ascent. Cranial is to the top, caudal to the bottom. Each letter (a-h) marks the origin of a spinal nerve root running from the spinal cord. Open rectangles symbolize vertebrae, large shaded rectangles (C and D) indicate the region of open SB lesion and small shaded rectangles (C and D) show the point of tethering of the spinal cord. The open arrow in (B) shows the direction of the physiological ascent of the spinal cord in normal fetuses while the single headed grey arrow in (D) shows the direction of the tethering force. The double headed grey

arrow in (D) shows the resulting stretching of the untethered closed spinal cord region immediately cranial to the SB. Note that the angulation of spinal nerves is *caudo*-lateral from spinal cord to ganglia in the normal fetus (B), but *cranio*-lateral in the SB fetus (D).

Europe PMC Funders Author Manuscripts